SCIENCE CHINA
Technological Sciences

• Article •

September 2021 Vol. 64 No. 9: 1927–1939
https://doi.org/10.1007/s11431-020-1760-3

A novel downshifting strategy based on medium-time-distance information for hybrid electric bus

CHENG Shuo[1], ZHANG Yan[2], YANG YiYong[2], FANG ShengNan[1*], LI Liang[1] & WANG XiangYu[1]

[1]*State Key Laboratory of Automotive Safety and Energy, Tsinghua University, Beijing 100084, China;*
[2]*School of Engineering and Technology, China University of Geosciences (Beijing), Beijing 100084, China*

Received August 28, 2020; accepted December 10, 2020; published online July 26, 2021

Vehicle downshifting during braking for the hybrid electric vehicle (HEV) equipped with the automatic mechanical transmission (AMT) could adjust work points of the motor. Thus, downshifting has great potential to effectively improve the efficiency of braking energy recovery. However, the power interruption during shifting could cause some loss of regenerative energy meanwhile. Hence, the choice of the downshifting point during vehicle braking which has crucial effect on energy recovery efficiency needs to be intensively studied. Moreover, the real-time application of the high-efficiency braking energy recovery strategy is a challenging problem to be tackled. Therefore, this paper proposes a dynamic-programming-rule-based (DPRB) downshifting strategy for a specific hybrid electric bus (HEB) driving condition. Firstly, the braking characteristic of the HEB during the process of pulling in is analyzed. Secondly, the medium-time-distance (MTD) demonstrating the dimension of time and space is proposed to define the boundary condition of the running bus. Then, look-up tables are established based on a dynamic programming algorithm offline using multiple sets of historical data. Thus, Based on the real-time driving data, whether to enter the optimal gear selection process can be decided online. Finally, simulations and hardware-in-the-loop (HIL) tests are carried out, and the results show that the proposed method can be indeed effective for braking energy recovery.

regenerative braking, medium-time-distance information, dynamic programming-rule based, hybrid electric bus

Citation: Cheng S, Zhang Y, Yang Y Y, et al. A novel downshifting strategy based on medium-time-distance information for hybrid electric bus. Sci China Tech Sci, 2021, 64: 1927–1939, https://doi.org/10.1007/s11431-020-1760-3

1 Introduction

Increasing fossil energy shortages and growing greenhouse effect put forward urgent requirements for more sustainable transportation [1–3]. As a key component of this paradigm shift, the hybrid electric vehicle (HEV) can pursue higher fuel economy than conventional vehicles merely equipped with internal-combustion-engine (ICE), and it has atrracted great concerns of academic and industrial circle worldwide [4–6]. Lots of new methods including improvement of regenerative braking control [7], optimization of energy management systems [8, 9], and raise of efficient transmission shifting strategies [10–13] have been studied all over the world.

A significant amount of energy consumed during braking could be recycled by regenerative braking for the HEVs/ electric vehicles (EVs) equipped with AMT, automatic transmission (AT), or double clutch transmission (DCT) [14], especially their frequent braking in urban bus driving conditions [15]. During the process of regenerative braking, the electric motor (EM) works as a generator to provide braking torque and generate electricity, and the regenerative energy is the power that the EM generates. In general, the common control method of a transmission tends to keep the gear position unaltered until the braking process is finished [16]. However, due to the high gear in the initial stage of braking, the power of the electric mechanism gradually may not

*Corresponding author (email: fsn@tsinghua.edu.cn)

meet the total braking force demand as vehicle speed decreases, which could cause loss of regenerative braking energy [17, 18]. Therefore, Li et al. [19] studied the braking energy recovery potential brought by downshifting with a dynamic programming (DP) algorithm. Additionally, in order to maximize braking energy recovery subject to braking stability while, Li et al. [20] proposed a particle swarm optimization (PSO) algorithm to deal with the optimization of braking energy recovery when antilock brake system (ABS) is triggered. The predictive method also shows extraordinary potential in the optimization of braking energy recovery. Xu et al. [21] proposed a non-linear model predictive regenerative braking control strategy for light electric vehicles equipped with in-wheel motors. With distribution coefficients of the braking force optimized off-line, Liu et al. [22] proposed an uncertainty predictive model to track the demand braking severity, Zou et al. [23] proposed a stochastic dynamic programming (SDP) algorithm based on a real-time Markov chain driver model. The neural dynamic programming (NDP) algorithm could be self-tuned with a wide variance in operating conditions [24]. Huang et al. [25] presented a review of model predictive control power management strategies for HEVs. In addition, artificial intelligence algorithms like neural networks and Fuzzy-logic-based regenerative braking strategies [26] have also been studied as well.

The above research mainly focused on optimal distribution of the braking force of electric machine and the pneumatic brake system (PBS) or hydraulic brake system (HBS) during the braking process. What is more, the studies on the real-time application and reliability due to the huge amount of computation are still insufficient, especially in urban public transport conditions with high security weights.

Therefore, this paper focuses on the downshifting strategy for a HEB, and proposes a method of combining high-efficiency braking energy recovery and the real-time application. The proposed method is based on the premise of the same city bus driving route conditions with a large number of repetitive features. Additionally, the proposed strategy is divided into two parts: (1) offline optimization of historical data with the DP, (2) online rule-based judgment based on current vehicle status. Furthermore, for different bus routes, as long as enough historical data can be obtained, the braking energy recovery efficiency can be optimized through the proposed strategy. The above-mentioned content is the main contribution of this paper. A HEB equipped with an AMT is studied in this research. Simulations are carried out to illustrate the benefit of downshifting implementation in braking energy recovery. At last, some simulation and hardware-in-the-loop (HIL) platform tests are established to verify the effectiveness of the proposed strategy.

The rest of the paper is as follows. Sect. 2 introduces the system dynamic models of the HEB. The braking process is analyzed and the downshifting strategy during bus arrival is introduced in Sect. 3. The descriptions of the simulation and HIL tests are given in Sect. 4. Results of simulations and HIL tests are given in Sect. 5. Sect. 6 presents the conclusion as well as suggestions for future research.

2 System dynamic models

This study focuses on a bus with a series powertrain topology. This HEV consistes of the following parts: a diesel engine, a clutch, an EM, an AMT and the braking system. These parts are shown in Figure 1.

2.1 Vehicle longitudinal dynamics model

When a vehicle runs on the ground, the driving resistance mainly contains vehicle rolling resistance and wind resistance. These resistances can be expressed by the following formul as

$$F_f = mg\cos\theta(f_0 + f_1\dot{x}), \tag{1}$$

$$F_{\mathrm{w}} = \frac{C_{\mathrm{D}}Av^2}{21.15}. \tag{2}$$

In eq. (1), F_f denotes the rolling resistance, m denotes the vehicle mass, f_0 and f_1 are the rolling resistance coefficients, v denotes the longitudinal speed of the vehicle, F_{w} denotes the wind resistance, C_{D} denotes the aerodynamic drag coefficient, θ denotes the road slope, and A is the vehicle frontal area.

Based on eqs. (1) and (2), the longitudinal dynamics equation of the vehicle is given as follows:

$$F_{\mathrm{resist}} = F_f + F_{\mathrm{w}}, \tag{3}$$

$$\frac{T_{\mathrm{w}}}{r} = \frac{T_{\mathrm{tq}}i_{\mathrm{g}}i_0\eta_T}{r} = F_{\mathrm{resist}} + mg\sin\theta + \delta m\frac{\mathrm{d}v}{\mathrm{d}t}, \tag{4}$$

where F_{resist} represents the total resist force, T_{w} denotes the total torque at each wheel, T_{tq} is the total demand torque, i_0

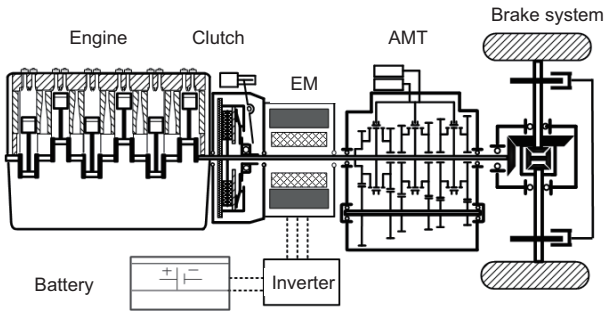

Figure 1 Schematic diagram of the HEV modeling system.

is the ratio of final drive and i_g is the ratio of AMT at the current gear position. η_T denotes the total efficiency of the mechanical transmission system, which can be divided into the efficiency of the final drive η_0 and the efficiency of the AMT η_g. θ denotes the road slope. δm denotes the correction coefficient of rotating mass.

2.2 Engine model

The fuel consumption per unit time of the diesel engine used in this paper can be expressed as

$$Q_g = \frac{P_e \cdot b_e}{367.1 \cdot \rho_g \cdot g}, \tag{5}$$

where ρ_g is the diesel density, and b_e denotes the fuel consumption rate per unit time, which is usually referred to as brake specific fuel consumption (BSFC). b_e is obtained from the engine power P_e and the engine rotational speed, as shown in Figure 2.

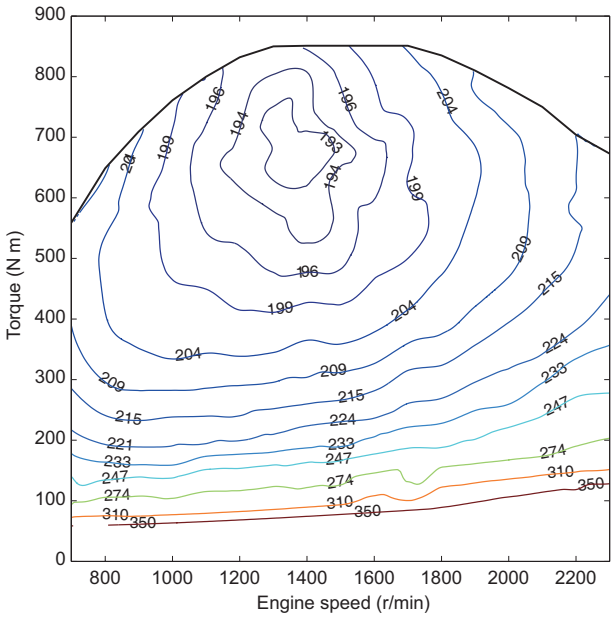

Figure 2 (Color online) Contour map of engine fuel consumption.

2.3 EM model

The dynamics of the EM is not concerned, so its model could be simplified as [27]

$$T_{EM} = \frac{T_{EM}^d}{1 + \tau_{EM} s}, \tag{6}$$

where the actual motor torque T_{EM} is calculate from the desired motor torque T_{EM}^d and the time delay constant τ_{EM}. In this paper, τ_{EM} is set to be 0.01 s.

The motor could work as a motor to provide the driving force or as a generator to recover energy. Therefore, the power calculation model could be defined as follows:

$$P_{EM} = T_{EM}\omega_{EM}\eta_{EM}^{\mathrm{sgn}(T_{EM})}, \tag{7}$$

where η_{EM} is the efficiency at current output speed ω_{EM}. The efficiency of the motor could be obtained from the current output speed and output torque based on the efficiency map, as shown in Figure 3.

The regenerative braking energy can be expressed as follows:

$$T_{reb} = \frac{T_{EM} \cdot i_0 \cdot i_g}{\eta_0 \eta_T}, \tag{8}$$

$$\omega_{EM} = i_0 i_g \frac{v}{r_\omega}, \tag{9}$$

where T_{reb} is regenerative braking torque. i_0 and i_g denote the ratio of the final drive and AMT. η_0 and η_T denote the efficiency of the final drive and the AMT, respectively. T_{reb} is the regenerative braking torque. r_ω denotes the radius of the tire.

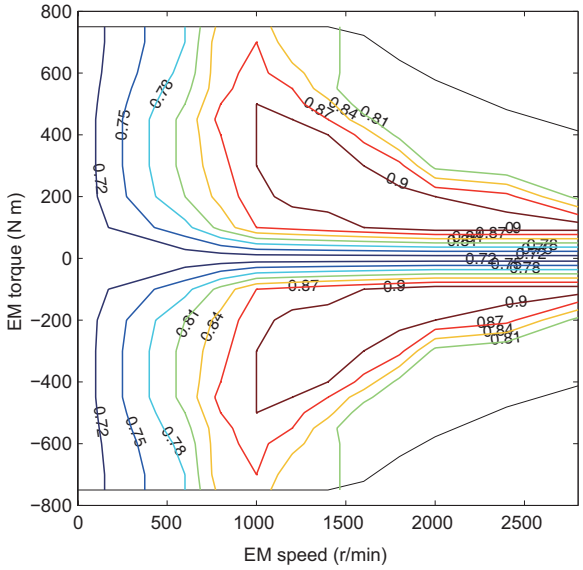

Figure 3 (Color online) Motor efficiency map.

2.4 Battery model and PBS model

The relationship between the state of charge (SOC) and other two parameters [28] is shown in Figure 4. Both too high and too low SOC could decrease the battery life [29], so the SOC must be restricted. Figure 4 shows that the charging resistance remains almost a constant when the SOC varied from 0.4 to 0.8, so this study regards the resistance as a constant and its value is 0.04. The initial SOC in this paper is set to be 0.6.

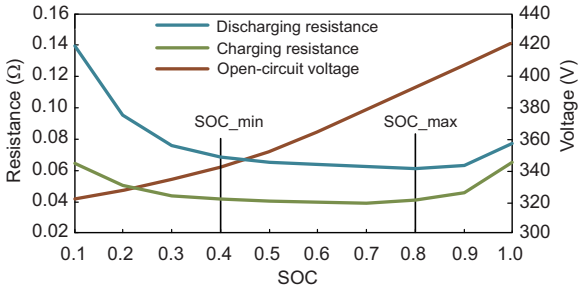

Figure 4 (Color online) Change curves of battery parameters.

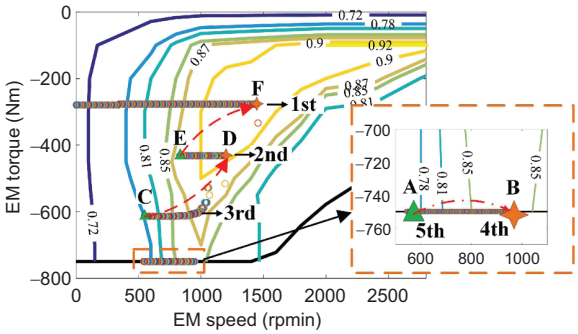

Figure 5 (Color online) Work points of EM change when shifting during regenerative braking process.

SOC increment expression can be written as follows:

$$\frac{\mathrm{dSOC}}{\mathrm{d}t} = \frac{V_{\mathrm{bat}} - \sqrt{V_{\mathrm{bat}}^2 - 4R_{\mathrm{bat}}P_{\mathrm{bat}}}}{2R_{\mathrm{bat}}Q_{\mathrm{bat}}}, \tag{10}$$

where V_{bat} denotes the open-circuit voltage, R_{bat} is the internal resistance, and Q_{bat} is the capacity of the battery.

The dynamic characteristic of PBS is not the focus of this paper. It is simplified as

$$T_{\mathrm{BP}} = \frac{T_{\mathrm{BP}}^d}{1 + \tau_{\mathrm{BP}}s}, \tag{11}$$

where T_{BP} and T_{BP}^d are the actual and desired PBS torque, respectively. τ_{BP} denotes the constant of the time delay. In this paper, τ_{BP} is set to be 0.015 s.

3 Design of the bus downshifting strategy while pulling in

This section describes the downshifting strategy proposed in this study.

3.1 Downshifting during braking process

The energy conservation of the regenerative braking process could be improved significantly if the AMT downshifts properly during the process of vehicle braking. A simulation with an initial velocity of (v=50 km/h) and a constant braking severity of (z=0.12) is carried out to intuitively demonstrate the improvement of the motor output efficiency due to downshifting. The rule-based strategy is used in this simulation [30]. When the vehicle decelerates, the AMT downshifting is advantageous in two situations, as shown in Figure 5.

When the braking power demand is greater than the upper power limit of the EM, the downshifting could improve the efficiency of the EM and slightly increase the output power of the EM. This is equivalent to an increased output power as a generator during the braking process. As shown in the Figure 5, the gear position is currently 5th (point A), and the efficiency of the EM is relatively low. If the AMT downshiftes to 4th gear position, the efficiency of motor can increase to point B, which means that the efficiency range of the motor can change from (0.81–0.85) to (0.85–0.9).

On the other hand, when the braking power is less than the upper limit of the EM power, the downshifting could improve the working efficiency of the EM without changing its output power. As shown in the Figure 5, the work point transfers from C (gear position: 3rd, efficiency: 0.85) to D (gear position: 2nd, efficiency: 0.9) and from E (gear position: 2nd, efficiency: 0.85) to F (gear position: 1st, efficiency: 0.9).

However, a power interruption during shifting exists, so that the rule-based downshifting strategy which does not consider the global optimization might not obtain the ideal energy recovery efficiency during the actual braking process. Therefore, it is necessary to carefully evaluate whether to downshift or not.

3.2 Data processing based on RMC and medium-time-distance information

With the continuous development of information technology, the cloud service of intelligent transportation systems (ITS) has made great progress and they generally include an offline part and an online part. A large amount of traffic flow data and vehicle status information can be recorded and saved offline. These data are obtained by the remote monitoring center (RMC), as shown in Figure 6.

The development of ITS can provide a powerful tool for buses to obtain more effective information. Then, the concept of medium-time-distance (MTD) based on the network architecture of an intelligent and connected vehicle is proposed, as shown in Figure 7. Fortunately, as we all know, intelligent and connected vehicle technologies including perception, decision, and control algorithm have been studied deeply, and many companies have devoted themselves to producing intelligent vehicles in recent years. Therefore, the proposed strategies can work in the intelligent bus in the future.

Figure 6 (Color online) The remote monitoring center (RMC).

The intelligent electric city bus is taken as an example. During the driving process of the bus, in addition to obtaining the bus's current status information, the surrounding environment could also be sensed through cameras, radars, a global positioning system (GPS), vehicle to everything (V2X) devices, and other devices [31]. Additionally, through the information exchange among the cloud server, the surrounding vehicles, and transportation facilities and so on, the bus can obtain traffic information such as the road gradient, traffic flows, pedestrians, and signal lights within a certain distance (100 m) ahead. Thus, the boundary conditions of the bus for a certain period of time (10 s) can be effectively predicted. These dimensions of time and space are named by the MTD information in this paper. As shown in Figure 7, MTD denotes the traffic situation in the near future and the space to be reached (between instantaneous prediction and overall planning).

In terms of bus routes in Chinese cities, the initial distance, initial acceleration, initial speed, and initial gear position when a bus is ready to dock at a bus stop, are all traceable due to speed limitations (≤ 60 km/h) and the existence of a large number of bus stations. Five drive cycles for extracting the data for the braking process are actually measured on the Chongqing No. 303 Bus route. The sequences of the recorded vehicle speed are shown in Figure 8. The vehicle seems to have similar velocity on the same road segment in different cycles. It can be seen from the Figure 8 that the vehicle speed is similar to the typical cycle condition of a form of Chinese urban public transport whose vehicle speed undergoes an approximate constant decline after experiencing an approximately constant rise.

In comparison with a car, the braking process of a bus is usually slow and mild due to a large number of repeated and regular bus driving conditions and the braking severity is usually smaller than 0.3 in each braking procedure, as shown in Figure 9. According to information from the MTD, the bus can obtain the road conditions ahead. Therefore, as long as no extremes (such as traffic accidents) occurr, the braking system will not trigger the antilock brake system (ABS). Therefore, the braking process of the bus stopping at the bus station can be regarded as a predictable, long-term, and light braking intensity deceleration condition, which is safe and promising for braking energy recovery.

3.3 DPRB-based real-time downshift strategy

The DPRB-based downshifting strategy of this study is shown in Figure 10, which is divided into two parts: (1) look-up-tables are established using multiple sets of historical data and a dynamic programming algorithm in the offline part; (2) the possibility of entering the optimal gear selection logic is judged by the vehicle status based on the current feedback.

3.3.1 Offline part

The offline part can be divided into three steps.

Firstly, the data for multiple bus travel times are obtained from the bus remote monitoring center (RMC), including driving time t corresponding to the driving speed v_t, gear position i_t, and road slope g_t.

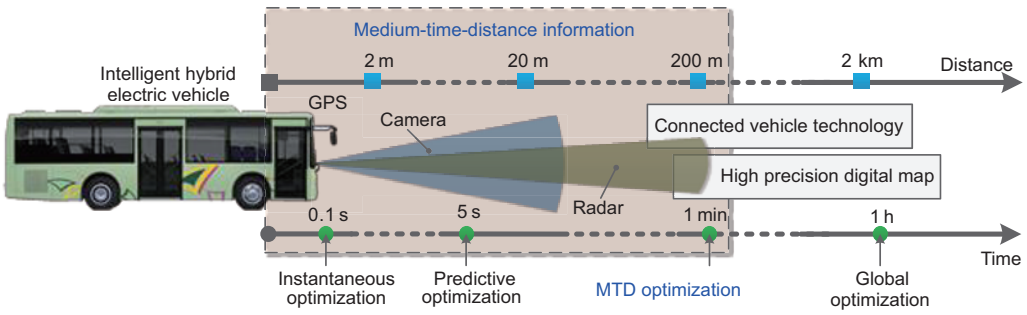

Figure 7 (Color online) Schematic diagram of the medium-time-distance concept.

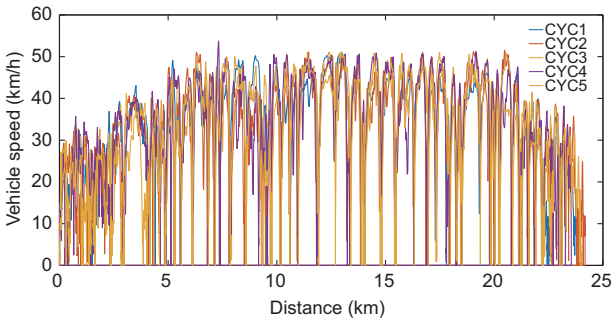

Figure 8 Velocity-distance curves in RMC.

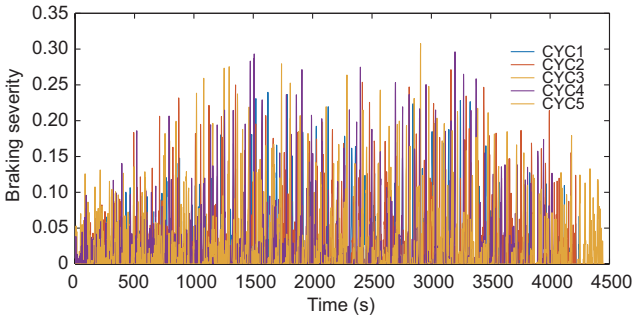

Figure 9 Braking severity-time curves of the driving cycles.

Secondly, multiple sets of braking conditions are screened out on the same bus route. In this study, different braking conditions are classified by different initial states based on a sufficient amount of experimental data, such as the initial vehicle velocity and the distance from the bus to the platform, as shown in Figure 11. P_n, d_{pn} and v_{pn} are station sequence, corresponding initial braking distance and initial braking speed, respectively.

All of the braking processes of the bus are divided into two categories in this study. The first process is the random braking process. Since the vehicle is traveling on a real road, complex traffic flow, signal lights, and pedestrians around also exist. Therefore, the braking condition of a relatively low initial speed due to random braking is excluded in the screening. In addition, deceleration and stopping of the bus at the station is a process that can be predicted by the driver, which is named

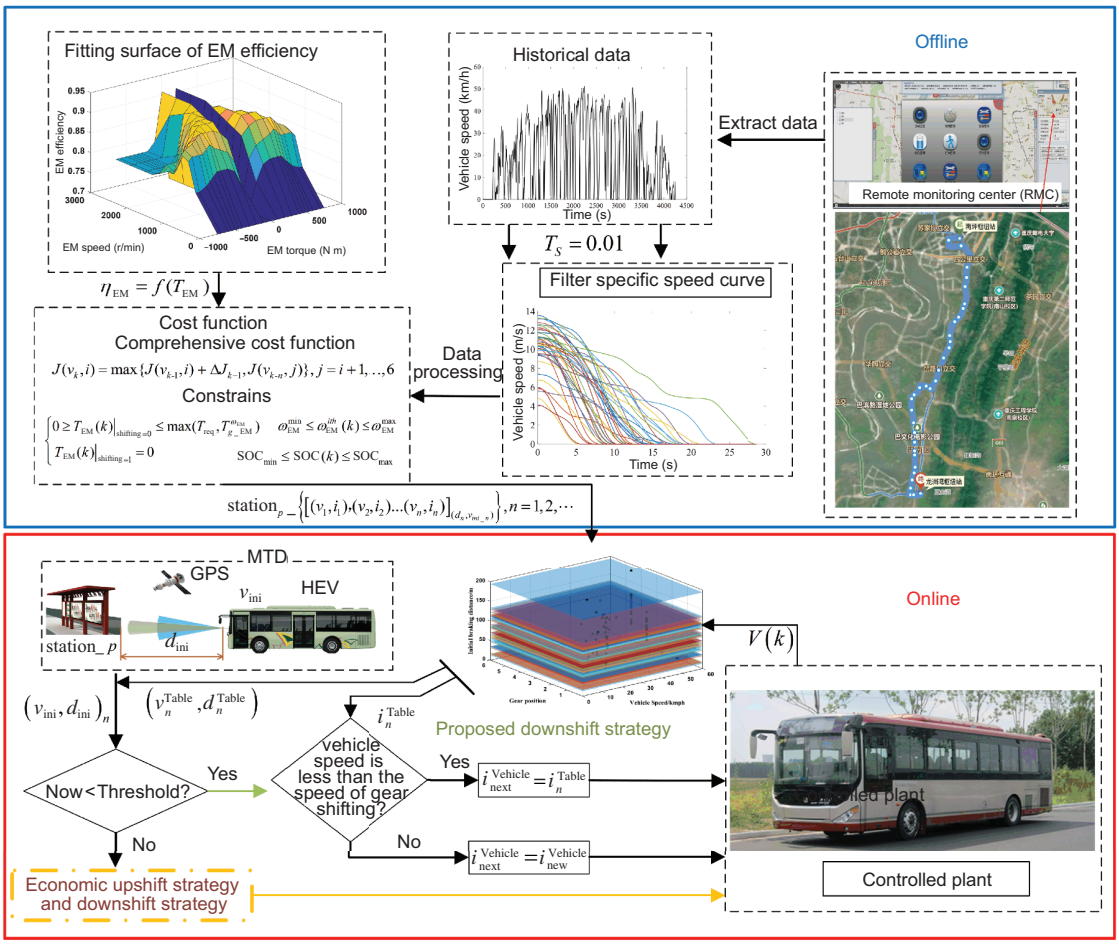

Figure 10 The logical diagram of the proposed downshifting strategy based on dynamic programming-rule based (DPRB) strategy.

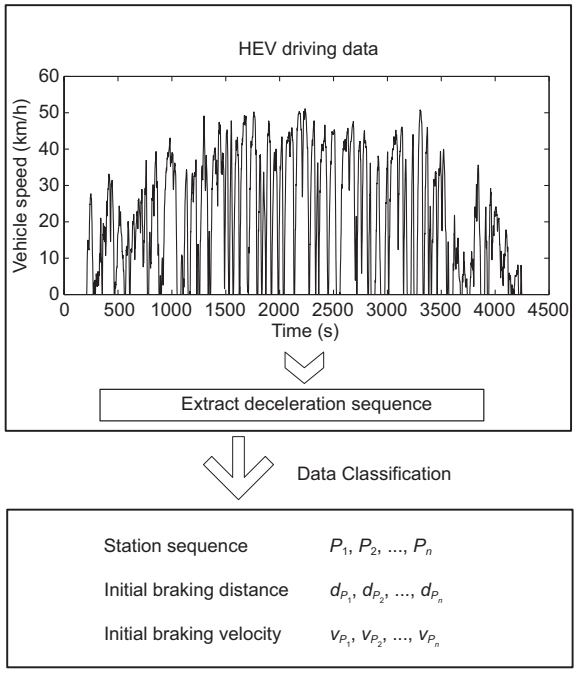

Figure 11 Flow chart of driving condition classification.

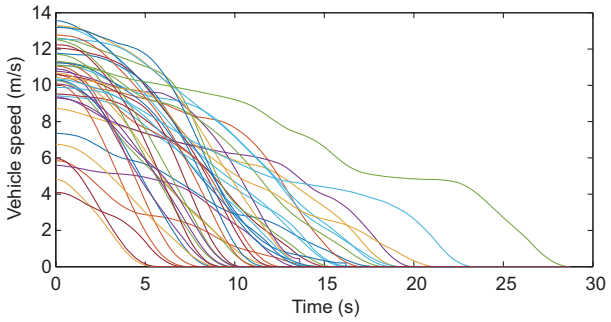

Figure 12 Deceleration curve for dynamic programming (DP) algorithm.

by the optimal downshifting process, and it is a process of slow deceleration for a relatively long time in general. Hence, only the data for braking conditions with the initial speed which is larger than 15 km/h and final speed which is smaller than 3 km/h for DP are collected in this study, as shown in Figure 12.

Thirdly, based on the station and its corresponding initial braking distance and initial velocity collected in Steps 1 and 2, the DP algorithm is used to extract the optimal downshifting speed point and the downshifting gear selection, which can be utilized online. The following shifting look-up-table is built, which could be delimited as

$$\text{station}_{p-}\left\{\begin{array}{l}[(v_1,i_1)(v_2,i_2)...(v_n,i_n)]_{(d_0,v_{ini\_1})},\\ [(v_1,i_1)(v_2,i_2)...(v_n,i_n)]_{(d_1,v_{ini\_2})},\\ \vdots\\ [(v_1,i_1)(v_2,i_2)...(v_n,i_n)]_{(d_n,v_{ini\_n})},\end{array}\right\}, \tag{12}$$

where station_p indicates the station where the bus stops after braking at the current moment, d_n denotes the initial braking distance, and i_n denotes the downshifting gear position when the current actual vehicle speed $v(k)$ is lower than downshifting threshold speed $v(n)$ in the recent future. The optimized downshifting speed point and gear selection of each deceleration curve which is shown in Figure 12 can be obtained through DP optimization. Each deceleration curve has a different number of downshifting points, which make up the above-mentioned shifting look-up-table.

The solution of the DP algorithm requires all the information of this process [32, 33], so it cannot be applied in real time. However, it can give the optimal solution for the optimization problem [34]. This study mainly focuses on braking energy recovery, so the recursion formula is defined as follows:

$$J(v_k,i)=\max\left\{J(v_{k-1},i)+\Delta J_{k-1},J(v_{k-n},j)\right\}, \tag{13}$$

where v_k is the vehicle speed at the current step, and vehicle speed at different stages can be defined as

$$v_{k-1}=v_k+z(v_{k-1})gT_s, \tag{14}$$

$$v_{k-n}=v_k+\sum_{s=k-n}^{k-1}z(v_s)gT_s, \tag{15}$$

where $T_s=0.01$ is the sample period of one step in Simulink. In dynamic programming algorithm of this study, speed is discretized into $v\in v^1, v^2, \ldots, v^{N_v}$. The initial $J(v_0,i_0)=0$, where v_0 and i_0 are the initial speed and initial gear position obtained from historical data by RMC. The other $J(v_n,i)$ value could also be originally set to be zero. The state (v_k,i) is attained in two ways. One way involves going from state (v_{k-1},i) to state (v_k,i) and the regenerative energy is

$$\Delta J_{k-1}=\int_{k-1}^{k}\Delta\text{SOC}\mathrm{d}t. \tag{16}$$

Another way involves going from state J_{k-n} to state J_k by making the choice to downshift , and the regenerative energy during this period is zero because of power interruption. The constraints are set as follows:

$$\text{s.t.}\left\{\begin{array}{l}0\le T_{\text{EM}}(k)|_{\text{shifting}=0}\le\max(T_{\text{req}},T_{g\_\text{EM}}^{\omega_{\text{EM}}}),\\ T_{\text{EM}}(k)|_{\text{shifting}=1}=0,\\ \omega_{\text{EM}}^{\min}\le\omega_{\text{EM}}^{ith}(k)\le\omega_{\text{EM}}^{\max},\\ \text{SOC}_{\min}\le\text{SOC}(k)\le\text{SOC}_{\max}.\end{array}\right. \tag{17}$$

Taking into account the shifting characteristics of the bus which is different from cars [30], it is considered in this study that power interruption period is equivalent to about 0.4 s when the algorithm chooses to downshift.

3.3.2 *Online part*

This study is focused on a braking energy recovery strategy that combines the obtained optimal solutions with real-time application capability. A rule-based strategy based on a look-up-table is used to ensure the real-time capability and reliability of downshifting during braking in an online module. For the automatic braking process, a hierarchical control architecture is designed, as shown in Figure 13.

Using the MTD information, the location of the bus at a specific moment and the distance between the bus and the next nearest station could be obtained. If the bus initial speed v_{ini} and distance d_{ini} between the bus and the station$_p$ are relatively smaller than the threshold speed v_{inin} and threshold distance d_n of the station as well as the braking pedal aperture is greater than zero at this time, optimal downshifting process will be triggered. In other cases such as the random breaking process and the acceleration condition, the AMT will follow the economic shifting strategy.

In the optimal downshifting process, the obtained real-time data are compared with the downshifting data stored in the vehicle control unit (VCU). Then, the downshifting speed point that is most suitable for this braking process will be selected. If the current vehicle speed $v(k)$ reaches the downshifting speed point, the VCU will send instructions to the transmission control unit (TCU), and then the TCU will command the AMT to downshift to the gear position j. If the current vehicle speed $v(k)$ does not reach the downshifting speed point, the VCU will send instructions to the TCU, and then, the TCU will command the AMT to remain the current gear position.

4 The description of simulation and HIL tests

To validate the performance of the proposed strategy, simulaitons and HIL tests are carried out. The difference of performance of two downshifting strategies in a single deceleration process is firstly analyzed based on MATLAB/Simulink. Then, a new set of 303 bus route cycle condition is selected to verify the performance on reducing fuel consumption of the DPRB strategy in the HIL bench. Moreover, the tested bus is a non-plug-in hybrid bus.

The simulation is one of the decelerations that triggers the optimal downshifting process. The initial bus velocity is 45 km/h, the end velocity is 0 km/h, the initial gear position is 4th, the initial SOC is 0.6, and the braking severity is a changing curve, as shown in Figure 14. Additionally, the results of three downshifting strategies used in the simulations will be discussed in the next section.

The experimental test bench is shown in Figure 15, and it consists of an AMT, three EMs, a clutch, and their electric control units (ECUs). The non-plug-in hybrid bus whose parameters are shown in Table 1 is used in the HIL tests, and it is established in Matlab/Simulink. The NI PXI is used as a host computer to communicate with ECUs by the controller area network (CAN). A flywheel is adopted for the inertia simulation. The proposed control algorithm is running on the host computer. The TCU sends the real-time gear position. Thus, the computer calculates and judges the vehicle status at that moment, then sends the next demand gear position to the TCU. A new driving cycle of the Chongqing No. 303 bus route is carried out as the test case. The results are shown in the next section.

5 Results and discussion

5.1 Downshifting process simulation

As shown in Figure 14, the entire braking process lasts about 10.2 s. With the rule-based strategy as shown in Figure 16(d), the AMT downshifts three times [4th, 3rd, 2nd, 1st]. The vehicle speeds of downshifting points are 36.73, 22.67, and 13.98 km/h. With the proposed strategy, the AMT downshifts

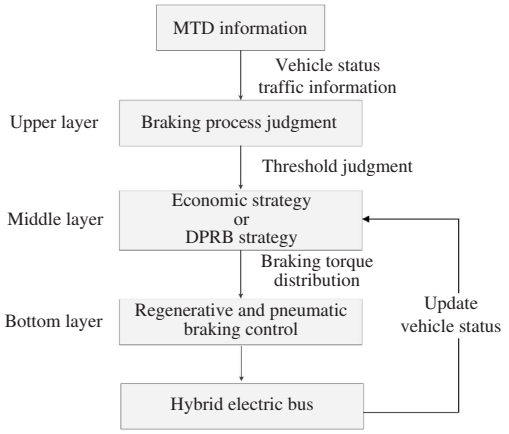

Figure 13 (Color online) MTD-based hierarchical control architecture for bus braking.

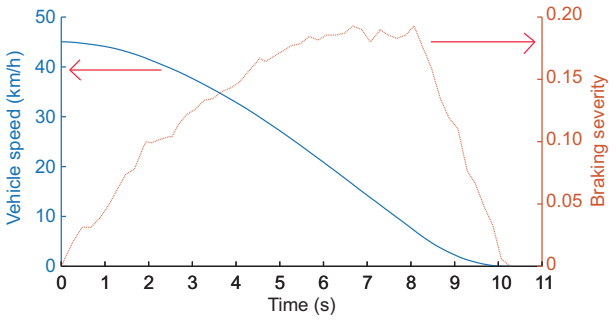

Figure 14 (Color online) Curves of speed-time and severity-time for simulation test.

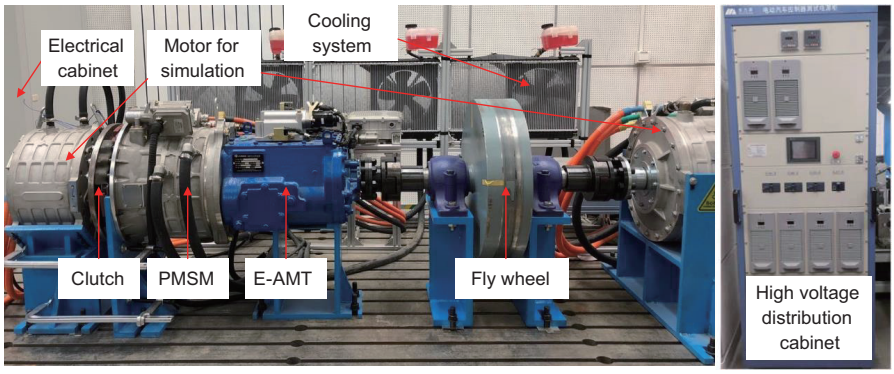

Figure 15 HIL platform for test.

Table 1 Results of simulation

Strategy	Final SOC	ΔSOC	Improvement
No-downshifting	0.6078	0.078	0
Rule-based	0.6084	0.084	7.7%
DPRB	0.6098	0.098	25.6%

only one time from 4th to 2nd, and the downshifting point is 27.49 km/h. Comparing with the three downshift modes, the above description is verified. That is to say, the efficiency of the motor is improved due to downshifting, but the power interruption caused by frequent downshifting will lead to reduce energy recovery. Therefore, comparing with the last two strategies, the EM operating torque of the proposed strategy is significantly higher in the entire braking interval. Additionally, as shown in Figure 16(b) and (c), when EM torque decreases sharply due to the power interruption, the pneumatic torque increases to compensate for the loss of EM braking torque, so that the desired braking torque could be maintained at the appropriate level and braking safety could be ensured.

Figure 17 also confirms the above statement. The increasing torque and efficiency of the EM due to downshifting results in greater SOC increments in a short period of time. However, due to the power interruption caused by frequent downshifting, the total SOC increment of the rule-based strategy is smaller than that of the proposed strategy.

As shown in Table 1, the increment of SOC is improved controlled by the downshifting strategies compared with that controlled by the no-downshifting strategy. Additionally, the

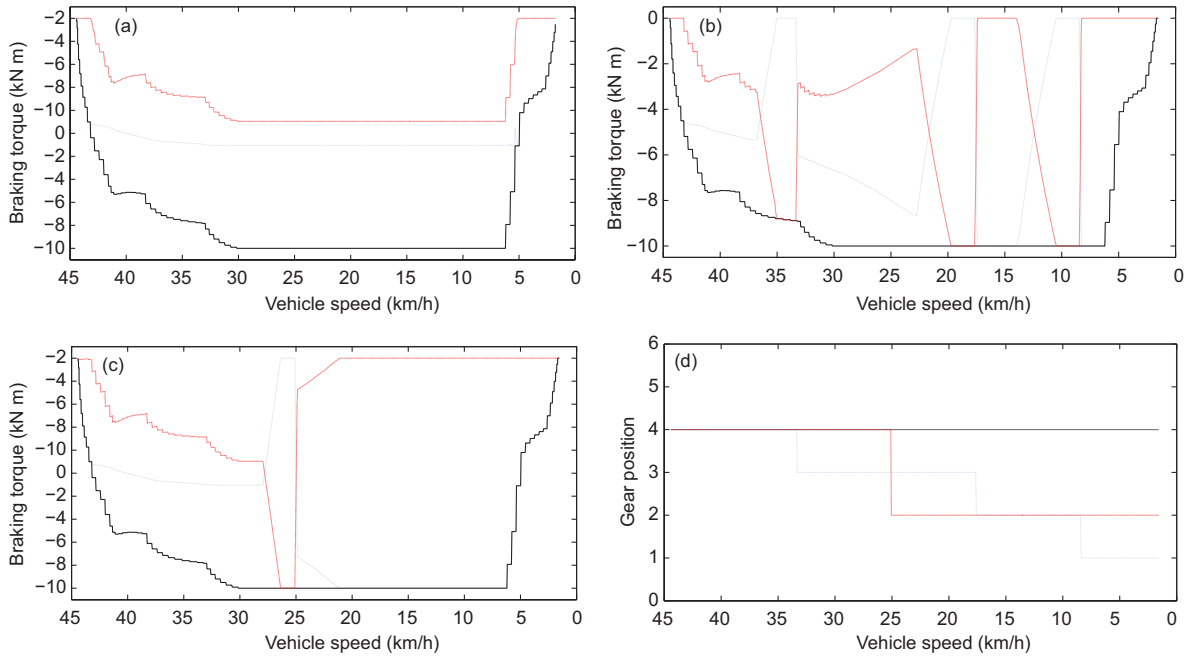

Figure 16 Torque distribution based on different strategies. (a) No-downshifting; (b) rule-based; (c) DPRB; (d) gear change under three strategies.

simulation results show that with the classic downshift strategy (the rule-based) and the proposed strategy, the regenerative braking energy is increased respectively by 7.7% and 25.6%, respectively.

5.2 Tests in HIL platform

Figures 18 and 19 demonstrate the results of HIL tests. As shown in Figure 18, the fuel consumptions controlled by different strategies are different. The fuel consumption analyzed in this paper has considered the change of SOC, and it can directly present the performance of different downshifting strategies because other operations of the test bus are consistent except the optimal downshifting processes. The fuel consumption rate of the entire process is the highest if the TCU chooses not to downshift, while the proposed strategy leads to the most fuel-efficient consequence. As shown in Figure 19(a), the wheel torque changes sharply because the gear position changes from the high gear position to the low gear position while the bus speeds up (the shifting strategy is

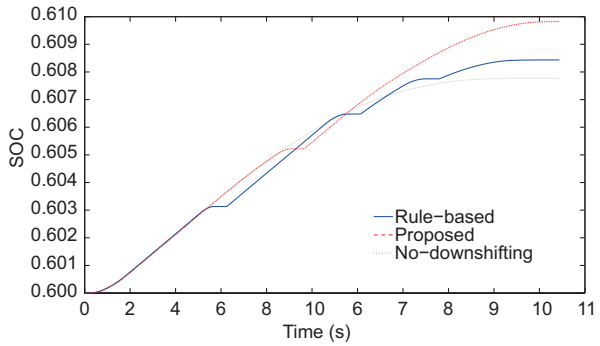

Figure 17 SOC curves of single braking process.

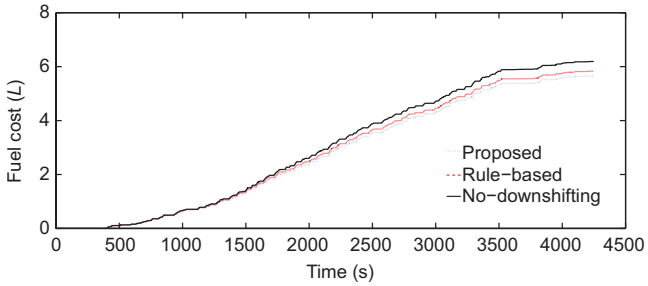

Figure 18 Fuel consumption of HIL test.

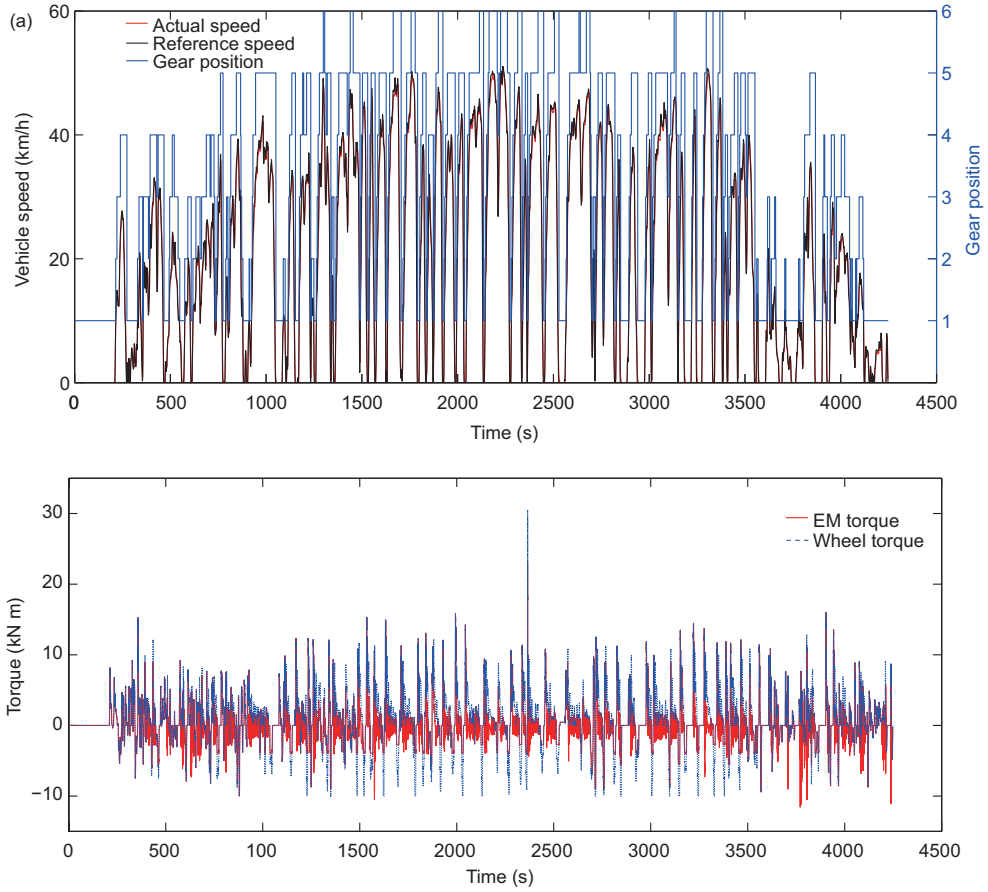

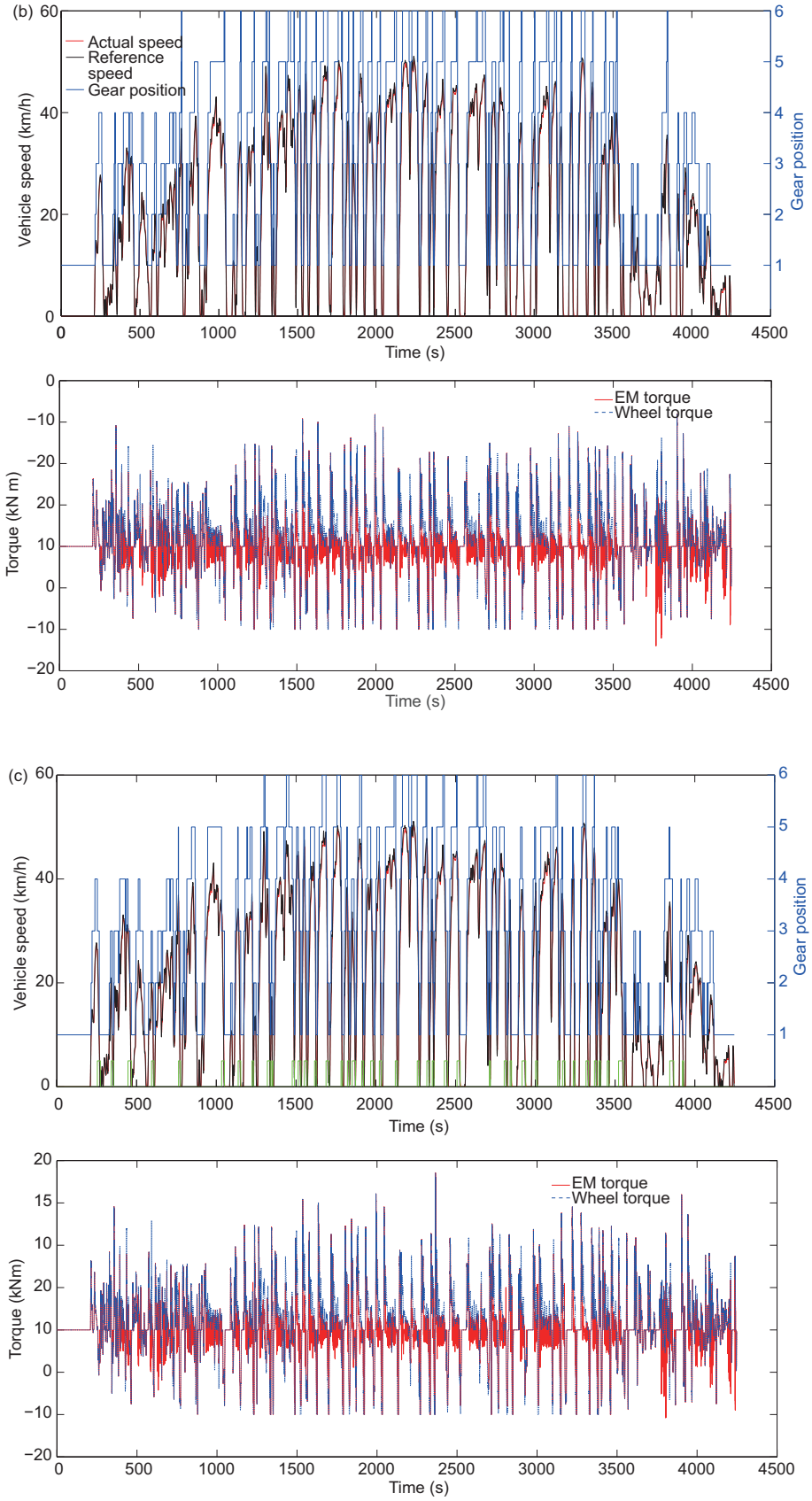

Figure 19 Results of no-downshifting (a), rule-based (b), and DPRB (c).

Table 2 Results of HIL test

Strategy	FC(L)	FC(L/100 km)	Improvement
No-downshifting	6.194	25.82	0
Rule-based	5.833	24.32	5.81%
DPRB	5.653	23.57	8.71%

changed from the no-downshifting strategy to the AMT general strategy). It can be seen in Figure 19(c) that the optimal downshifting process is triggered about 42 times. As shown in Table 2, with the proposed strategy, the fuel consumption is reduced by 8.71%, which is 3% higher than that of the Rule-based strategy.

6 Conclusions

In order to combine the optimization of braking energy recovery efficiency with the real-time applicability of the algorithm, a HEB equipped with AMT is taken as a research subject in this study. The DP-based strategy could not be processed without the global information, and the rule-based strategy does not have ideal optimization efficiency. However, for bus routes with a large number of repetitive conditions and fixed parking locations, a compromise and a practical application potential method is found in this study. The practical application potential method uses historical data optimized by DP to create look-up-tables offline, and it uses the rule judgment as well as looking up existing tables online to handle these two issues. So for, n terms of similar transportation modes such as urban buses with repeated routes and working conditions, this study provides a practical and feasible braking energy recovery scheme.

The simulation results of the single braking process show that with the DBRB strategy proposed by this study, the regenerative energy can be increased by 25.6% compared with the no-downshifting strategy. The fuel consumption is reduced by 8.71% with the proposed strategy in the HIL test.

Future work could research further the following issues. One aspect is that this algorithm should be improved to extend its application to vehicles with similar driving conditions, such as intelligent logistics vehicles with repeated routes and fixed travel times. Another aspect is that the computational burden of the optimization algorithm may be further reduced by studying some learning methods of optimizing the offline storage space.

This work was supported by the National Natural Science Foundation of China (Grant Nos. 51975048 and 51805290).

1 Krithika V, Subramani C. A comprehensive review on choice of hybrid vehicles and power converters, control strategies for hybrid electric vehicles. Int J Energy Res, 2018, 42: 1789–1812
2 Takeshita T. Assessing the co-benefits of CO_2 mitigation on air pollutants emissions from road vehicles. Appl Energy, 2012: 97: 225–237
3 Dincer I, Rosen M A. The roles of science and technology in energy and environment research and development. Int J Energy Res, 2001, 25: 1165–1187
4 Ehsani M, Gao Y, Emadi A. Modern Electric, Hybrid Electric, and Fuel Cell Vehicles Fundamentals, Theory, and Design. 2nd ed. Boca Raton: CRC Press, 2010
5 Grimaldi C N, Lunghi P, Mariani F. Energy saving strategies in an actual confectionery plant. Int J Energy Res, 2000, 24: 769–777
6 Pei J Z, Su Y X, Zhang D H, et al. Velocity forecasts using a combined deep learning model in hybrid electric vehicles with V2V and V2I communication. Sci China Tech Sci, 2020, 63: 55–64
7 Hu X, Murgovski N, Johannesson L M, et al. Comparison of three electrochemical energy buffers applied to a hybrid bus powertrain with simultaneous optimal sizing and energy management. IEEE Trans Intell Transp Syst, 2014, 15: 1193–1205
8 Pei J Z, Su Y X, Zhang D H. Fuzzy energy management strategy for parallel HEV based on pigeon-inspired optimization algorithm. Sci China Tech Sci, 2017, 60: 425–433
9 Zhang Z, Zhang X, Pan H, et al. A novel steering system for a space-saving 4ws4wd electric vehicle: Design, modeling, and road tests. IEEE Trans Intell Transp Syst, 2017, 18: 114–127
10 Hu J, Jiang X, Zheng L. Design and analysis of hybrid electric vehicle powertrain configurations considering energy transformation. Int J Energy Res, 2018, 42: 4719–4729
11 Yi C, Epureanu B I, Hong S K, et al. Modeling, control, and performance of a novel architecture of hybrid electric powertrain system. Appl Energy, 2016, 178: 454–467
12 Tian H, Lu Z, Wang X, et al. A length ratio based neural network energy management strategy for online control of plug-in hybrid electric city bus. Appl Energy, 2016, 177: 71–80
13 Li L, Yang C, Zhang Y, et al. Correctional DP-based energy management strategy of plug-in hybrid electric bus for city-bus route. IEEE Trans Veh Technol, 2015, 64: 2792–2803
14 Hu X, Martinez C M, Yang Y. Charging, power management, and battery degradation mitigation in plug-in hybrid electric vehicles: A unified cost-optimal approach. Mech Syst Signal Process, 2016, 87: 4–16
15 Liu B H, Li L, Wang X Y. Hybrid electric vehicle downshifting strategy based on stochastic dynamic programming during regenerative braking process. IEEE Trans Vehicular Tech, 2018, 67: 4716–4727
16 Oleksowicz S A, Burnham K J, Southgate A, et al. Regenerative braking strategies, vehicle safety and stability control systems: Critical use-case proposals. Vehicle Syst Dyn, 2013, 51: 684–699
17 Zhao Z G, Li X Y, Wu C C. Optimal control in brake down-shifting process for hybrid electric car equipped with dry dual clutch transmission. Sci Sin Tech, 2016, 46: 950–960
18 Zhao Z, Chen J, Li X, et al. Downshift decision and process optimal control of dual clutch transmission for hybrid electric vehicles under rapid braking condition. Mech Syst Signal Process, 2019, 116: 943–962
19 Li L, Li X, Wang X, et al. Analysis of downshift's improvement to energy efficiency of an electric vehicle during regenerative braking. Appl Energy, 2016, 176: 125–137
20 Li L, Zhang Y, Yang C, et al. Model predictive control-based efficient energy recovery control strategy for regenerative braking system of hybrid electric bus. Energy Convers Manage, 2016, 111: 299–314
21 Xu W, Chen H, Zhao H Y, et al. Torque optimization control for electric vehicles with four in-wheel motors equipped with regenerative braking system. Mechatronics, 2019, 57: 95–108
22 Liu W, He H, Guo H, et al. Control research for hybrid compound braking based on an uncertainty predictive model. 2014, doi:

10.1109/ITEC-AP.2014.6941108
23 Zou Y, Kong Z, Liu T, et al. A real-time markov chain driver model for tracked vehicles and its validation: Its adaptability via stochastic dynamic programming. IEEE Trans Vehicular Tech, 2017, 66: 3571–3582
24 Li W, Xu G, Xu Y. Online learning control for hybrid electric vehicle. Chin J Mech Eng, 2012, 25: 98–106
25 Huang Y, Wang H, Khajepour A, et al. Model predictive control power management strategies for HEVs: A review. J Power Sources, 2017, 341: 91–106
26 Zhang J M, Song B Y, Cui S M, et al. Fuzzy logic approach to regenerative braking system. In: Proceedings of the International Conference on Intelligent Human-Machine Systems and Cybernetics. Hangzhou, 2009. 451–454
27 Wang X, Li L, Yang C. Hierarchical control of dry clutch for engine-start process in a parallel hybrid electric vehicle. IEEE Trans Transp Electrific, 2016, 2: 231–243
28 Guo H Q, Wang X Y, Li L. State-of-charge-constraint-based energy management strategy of plug-in hybrid electric vehicle with bus route. Energy Conversion Management, 2019, 11: 111972
29 Zou Y, Hu X, Ma H, et al. Combined state of charge and state of health estimation over lithium-ion battery cell cycle lifespan for electric vehicles. J Power Sources, 2015, 273: 793–803
30 Li L, Wang X, Xiong R, et al. AMT downshifting strategy design of HEV during regenerative braking process for energy conservation. Appl Energy, 2016, 183: 914–925
31 Flah A Mahmoudi C. Design and analysis of a novel power management approach, applied on a connected vehicle as v2v, v2b/i, and v2n. Int J Energy Res, 2019, 43: 6869–6889
32 Zhang S, Xiong R. Adaptive energy management of a plug-in hybrid electric vehicle based on driving pattern recognition and dynamic programming. Appl Energy, 2015, 155: 68–78
33 Yang Y, Hu X, Pei H, et al. Comparison of power-split and parallel hybrid powertrain architectures with a single electric machine: Dynamic programming approach. Appl Energy, 2016, 168: 683–690
34 Zhang S, Xiong R, Sun F. Model predictive control for power management in a plug-in hybrid electric vehicle with a hybrid energy storage system. Appl Energy, 2017, 185: 1654–1662